Improving Deep Sensitivity of Four-Electrode Focused Impedance Method In Lungs by Varying Electrode Geometries

Mahjabin Mobarak[1,2] and K Siddique-e Rabbani[3]

1. Center for Higher Studies and Research, Bangladesh University of Professionals Dhaka, Bangladesh.
2. Department of Electrical and Electronics Engineering, Fareast International University, Dhaka, Bangladesh.
3. Department of Biomedical Physics & Technology, University of Dhaka, Dhaka 1000, Bangladesh.

Email: ahmedmahjabin@gmail.com

ABSTRACT

Bio-Electrical impedance is of special interest in the detection and diagnosis of lung problems, particularly in the low and medium income countries. An age old simple technique employing four electrodes is known as 'Tetra Polar Impedance Measurement (TPIM)' but it cannot localize a particular zone of interest region. A new technique named as 'Focused Impedance Method (FIM)' was innovated by a Dhaka University group which gives high sensitivity in a localized zone of interest. Previously FIM was used from one side of the thorax which gave a rather limited information from the lungs, from shallow depths only. In order to get information from deeper regions of the lungs a new configuration of electrodes for FIM was proposed by the same group at Dhaka University which placed two electrodes at the front and two electrodes at the back of the thorax in a horizontal plane. It is expected that the degree of depth sensitivity would depend on electrode separation on both the sides. The electrode width may also have an effect. In order to study these quantitatively, COMSOL Multiphysics software was used to simulate the measurements in a rounded rectangular volume to represent a typical thorax, which was filled with isotonic saline. Electrode separations of 5cm, 10cm, 15cm and 20cm were studied while electrode widths studied were 0.15cm, 1cm and 3cm. The work supported the proposed new configuration of electrodes for FIM in that this method gives enhanced sensitivity throughout the depths of a lung and that for a thorax with a cross section of 33cm×26cm, an electrode separation between 10cm and 15cm would give optimum results. For electrode width, the ones studied did not give any significant difference, however, the smallest (0.15cm) one appeared to give slightly better results.

Key words: Bioelectrical Impedance, TPIM, FIM, Lungs, Deep Sensitivity.

1. INTRODUCTION

Scientists all over the world are trying to innovate simple, inexpensive, and non-invasive techniques for the physiological study and diagnosis of the human body. Electrical impedance techniques play a very significant role in this regard (Morucci and Rigaud, 1996, Rabbani and Kadir, 2011). Individual body tissues have various electrical properties which can change due to physiological changes or due to sickness (Gabriel et al.,1996). Electrical impedance estimation has been a chosen procedure for observing the condition of tissues or organs since it is non-invasive, cheap, and simple (Khalil et al., 2014). Two significant important electrical properties are shown in biological tissues: electrical conductivity because of free charge, and dielectric properties (in

the form of permittivity) because of bound charge (Thomasset, 1963). Electrical impedance therefore, portrays the conditions of the relative electrical conductivity and permittivity and thus has the potential for distinguishing inhomogeneity inside the body (Lingwood et al., 1999).

For bio-impedance measurements using skin surface electrodes, Tetra-Polar Electrical Impedance Measurement (TPIM) is normally used since it eliminates the contact impedance which may be significantly high compared to that of the internal bulk of the body. In typical TPIM, a pair of electrodes is used to drive an alternating current (AC) of constant amplitude into a volume conductor and the resulting voltage is measured across another electrode pair. The ratio of the measured voltage to the driven current gives the transfer impedance of the volume conductor for a particular electrode configuration (Geselowitz, 1971) However, simple TPIM has a wide zone of sensitivity and cannot localize a specific region within the body. Therefore, its application remained limited although it was conceived and developed a long time back (Redisch, 1970).

EIT (initially named Applied Potential Tomography), developed in the 1980s allowed localization of electrical impedance through an impedance distribution in a 2D plane and created a great deal of interest (Barber et al., 1984). However, EIT requires many electrodes, complex instrumentation with computerized data acquisition and sophisticated algorithms, making the device potentially expensive. Besides, it is still going through a development stage and has not come to the regular clinical application area as yet.

Focused Impedance Method (FIM), an innovation of our extended group at the University of Dhaka is a bridge between TPIM and EIT where two TPIM measurements are carried out orthogonally around a central zone of interest (Rabbani et al., 1999, Rabbani and Karal, 2008, Rabbani, 2018a). The sum of the transfer impedances has enhanced sensitivity within the central zone and hence can measure the change in transfer impedance of a specified target zone within a volume conductor minimizing the contribution from the neighboring zones (Islam et al. 2010). Most of the studies done so far using FIM used electrodes on one side of the body having sensitivity down to a small depth.

Recently Rabbani (2018b) proposed several configurations of electrodes for probing deep regions inside the body, targeting different organs of interest. One of these used four electrodes with two in the front of the body and two at the back, along a horizontal plane as shown in Figure 1. In this technique, firstly, two individual measurements for TPIM are performed configuring current drive electrodes (I) and potential measuring electrodes (V) as shown in Figures 1*a* and 1*b* respectively. These create distributions of sensitivity that are essentially orthogonal to each other which are represented qualitatively through shades of red in these figures. Figure 1*c* shows the expected result when these two distributions are combined through an algebraic addition, which essentially gives the FIM, in which the central region is expected to have a higher effective sensitivity. This configuration was suggested for targeting the lung region. Using this configuration, Mobarak and Rabbani (2019) performed simulated sensitivity measurements using COMSOL software package (COMSOL, 2022) which supported the prediction. Strictly speaking, an average of the two TPIM

values are to be taken for FIM, However, to compare relative sensitivity distributions, an addition of the two TPIM values may be used as well.

In the previous work by Mobarak and Rabbani (2019) a fixed electrode separation (ES) of 15 cm was used. The sensitivity distribution is expected to change with the geometry of the electrodes, particularly the ES in the front and the back, the width of the electrodes, etc., which need to be studied in order to obtain an optimized configuration to focus a target lung, either left or right. The present work was taken up to answer these questions.

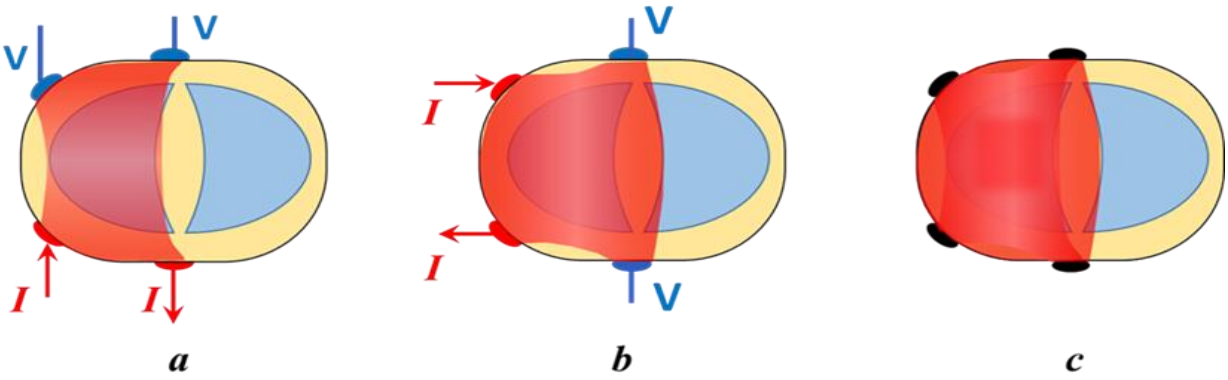

Fig. 1: Simplified schematic sensitivity portrayal of a transverse cross-section of volume conductor for square TPIM (a, b) with electrodes in the front and back of the thorax. The current drive electrodes (red dots) and the potential electrodes (blue dots) are shown in each diagram for the respective TPIM configurations. The figure on the right (c) shows an expected sensitivity portrayal for FIM which is an average of the sensitivity distributions of the two TPIMs (Rabbani, 2018b). FIM is expected to give a high sensitivity in the central region.

2. MATERIALS AND METHODS

To study the new configurations of electrodes a rounded rectangular box (phantom) of dimension 33cm×26cm×12cm, as schematically depicted in Figure 2(a) was simulated in COMSOL. In future, an experimental verification of the simulation results was planned using a similar box filled with saline. The choice of the phantom dimensions and the electrodes was guided by this requirement. For the first study, cylindrical rod shaped metal electrodes of 0.3cm diameter and with a length of 3cm were attached inside the walls of the front and back of the box, centered about line PQ in Figure 2(b). The electrode separation (ES) between the pair on the front and the back were taken as 5cm, 10cm, 15cm, and 20cm respectively for this study. For the other study, flat electrodes were used with a thickness of 0.15cm and the widths of the electrodes were taken as 0.15cm, 1cm, and 3cm respectively. The length of the electrodes was kept fixed at 3cm as before. The distance between the left edge and the central line PQ between the electrodes was kept fixed at 20.5cm as shown. The electrode material was chosen as stainless steel with a conductivity of 1.4×10^6 S/m and a relative permittivity of 1. This box was filled up with 0.9% isotonic saline with

a conductivity of 1.2 S/m and relative permittivity of 80 (Sauerheber and Heinz 2015). The current drive frequency was chosen at 1 kHz.

The scheme of measurement of FIM is explained with the help of Figure 2(b). The four electrodes are indicated by A, B, C, and D. In the first step of FIM measurement, a TPIM measurement (TPIM-1) is carried out with current driven through electrodes C & D while the potential is measured across electrodes A & B. In the second step, another TPIM measurement (TPIM-2) is carried out with current driven through electrodes B & D while the potential is measured across electrodes A & C. For each, the respective transfer impedances are computed. In the third step, the above two TPIMs (TPIM-1 and TPIM-2) are added (or averaged) to give FIM.

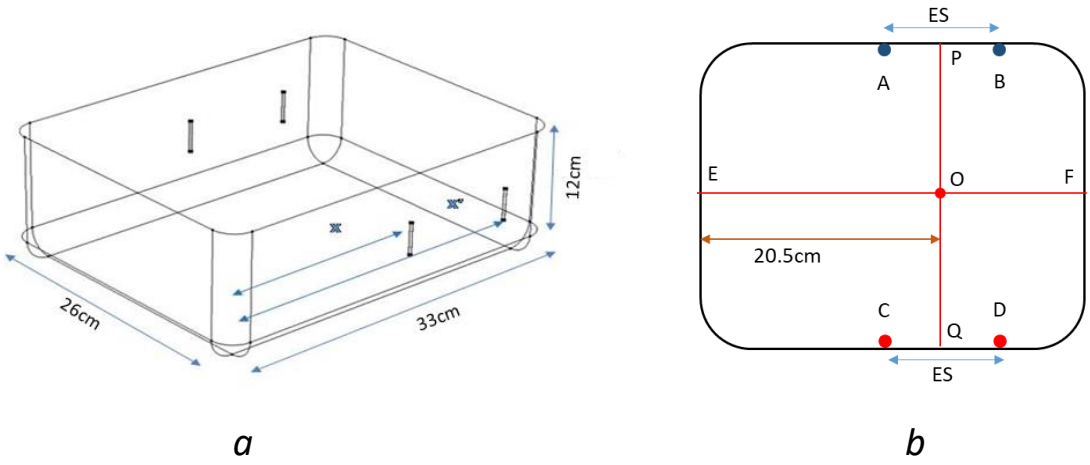

Fig. 2: (a) 3D schematics of 4-electrode configuration in a rectangular box (phantom) with both sided electrode placements. (b) Cross-sectional view showing scheme for 4-electrode FIM.

In the present work, the sensitivity distributions within the box for TPIM-1, TPIM-2, and FIM were obtained using COMSOL. The sensitivity distributions were displayed as colored contour images. The numerical sensitivity values at the centre point 'O' in Figure 2(b) for the different configurations were then compared for the different electrode configurations.

In order to obtain the point sensitivity *S* for a particular TPIM configuration, the transfer impedance was obtained using the following equation (Grimnes and Martinsen, 2014).

$$S = \frac{J_1 \cdot J_2}{I^2} \qquad \ldots\ldots\ldots (1)$$

Where $\boldsymbol{J_1}$ and $\boldsymbol{J_2}$ are the current density vectors at that point due to a fixed current of magnitude I driven between the current drive electrode pair and the potential electrode pair respectively. Here, I^2 in the denominator normalizes the sensitivity.

In 4-electrode FIM, since the current and potential electrodes are interchanged orthogonally and the results added, the resulting point sensitivity will be given by the addition of the two appropriate point sensitivities for two TPIM configurations, following equation 1. Thus if $\boldsymbol{J_1}$, $\boldsymbol{J_2}$, $\boldsymbol{J_3}$, and $\boldsymbol{J_4}$ are the current density vectors at a point within the volume conductor for injection of current *I* through the electrode pairs (A-B) & (C-D) for TPIM-1 and (A-C) & (B-D) for TPIM-2, then the FIM sensitivity at any point is given by,

$$FIM\ Sensitivity = \frac{\boldsymbol{J_1 \cdot J_2 + J_3 \cdot J_4}}{I^2} \quad \ldots (2)$$

In the COMSOL model, an alternating current of unit amplitude (1A) was injected through the electrode pairs (A-B), (C-D), (A-C), and (B-D) simultaneously using the electric current interface in AC/DC module. For a visualization of FIM sensitivity distribution, colour contour distribution was used. To compare the different electrode configurations numerically, the value of sensitivity at point O in Figure 2b was used.

3. RESULTS AND OBSERVATIONS

3.1 Effect of electrode separation (ES)

Table 1 shows the sensitivity at the center point (O in Figure 2b) of the electrode configuration for the different electrode separations, showing the individual TPIM values as well as the resulting FIM value. The FIM value is shown both as added and as averaged values of the two corresponding TPIM values.

Table 1: Sensitivity at the center of the electrode configuration for different electrode separations (ES)

ES, cm	Sensitivity, arbitrary unit			
	TPIM-1 (A-B) & (C-D)	TPIM-2 (A-C) & (B-D)	FIM added	FIM averaged
5	89	1202	1291	646
10	290	990	1280	640
15	508	754	1266	633
20	668	569	1237	619

It may be seen that at the centre point of the electrode configuration, the sensitivity value for TPIM-1 increases with electrode separation while that for TPIM-2 decreases with electrode separation. Values for FIM decrease very little with electrode separation, which is an advantage.

Color sensitivity distributions of 4-electrode FIM for a horizontal plane at the vertical centre of the rectangular phantom are shown in Figure 3 for different ES. Since the sensitivity values are very high close to the electrodes which are not of much importance to most of the studies in practice, the sensitivity range has been truncated appropriately to show desirable features. The positive sensitivity values are shown in light green (low value) through yellow and red to dark brown (high value). Negative sensitivity values are shown in shades of blue; light blue for a low value and deep blue for a high value.

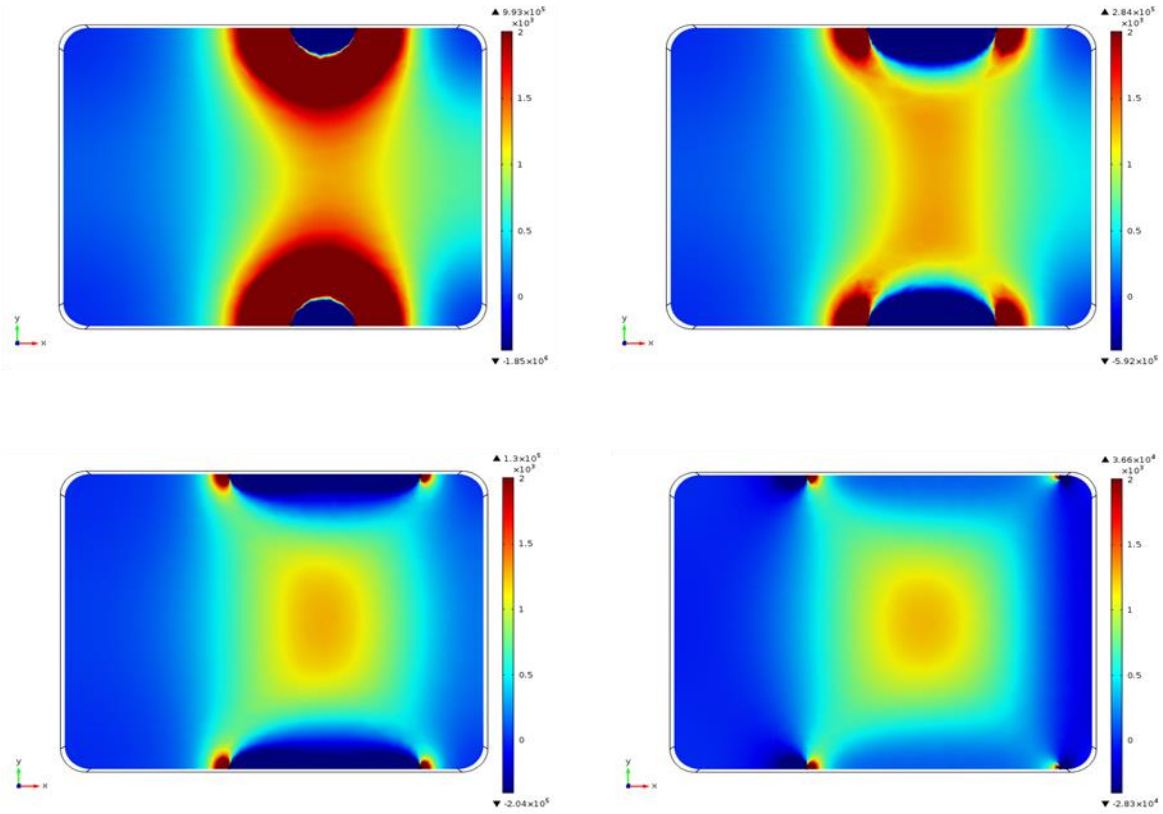

Fig. 3: Sensitivity distribution of 4-electrode FIM at mid height (6cm) for different ES; top left: 5cm, top right: 10cm, bottom left: 15cm, bottom right: 20cm. Sensitivity range truncated beyond the values of −400 and +2000 in arbitrary units as obtained through the simulation.

Figure 4 plots the sensitivity of FIM along the width (line PQ in Figure 2b) for different electrode separations. It may be observed that the sensitivity becomes more uniform with increasing ES along with a decrease in negative sensitivity. There is no negative sensitivity for an ES of 20cm.

Figure 5 shows the sensitivity of FIM along the length of the box (line EF in Figure 2b) at the midpoint of the width (13cm from Q) for various ES. It may be observed that all the plots have peaks at around 20.5cm, which is the centre point of all the electrode configurations, with very low values outside the region of interest bounded by the electrodes. Interestingly, here, the 20cm ES shows negative sensitivity outside the central region, while none of the plots for other ES show

negative sensitivity. From a combined assessment of Figures 4 and 5, an ES value of 15cm was taken to be optimum for this phantom and further studies on the effect of electrode width were performed using this value of electrode separation.

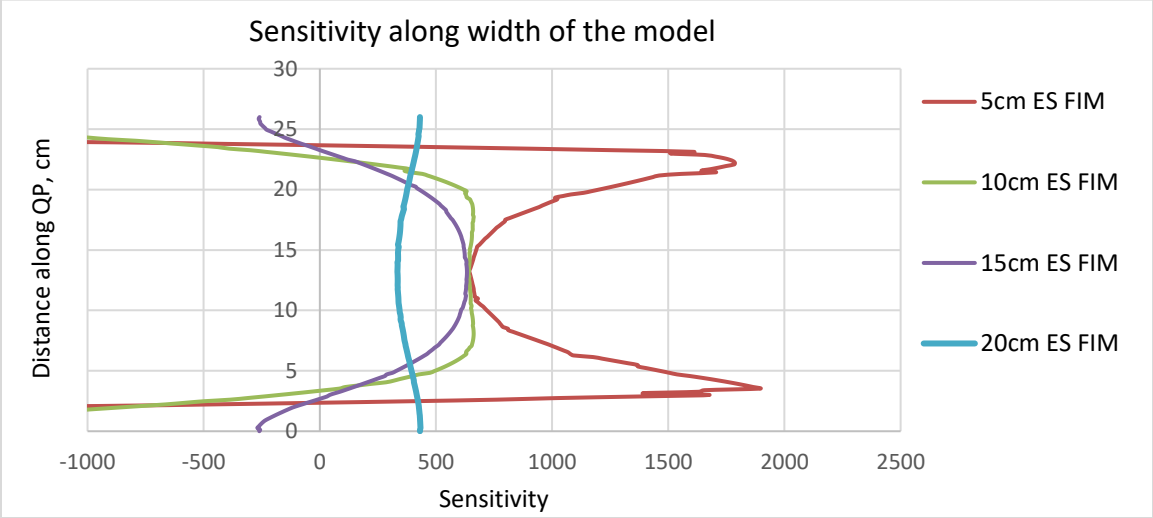

Fig. 4: Sensitivity of FIM (added) along the width (PQ) of the phantom for various ES. Vertical axis shows distance from point Q, along QP. The sensitivity becomes more uniform with increasing ES with decrease in negative sensitivity. There is no negative sensitivity for an ES of 20 cm.

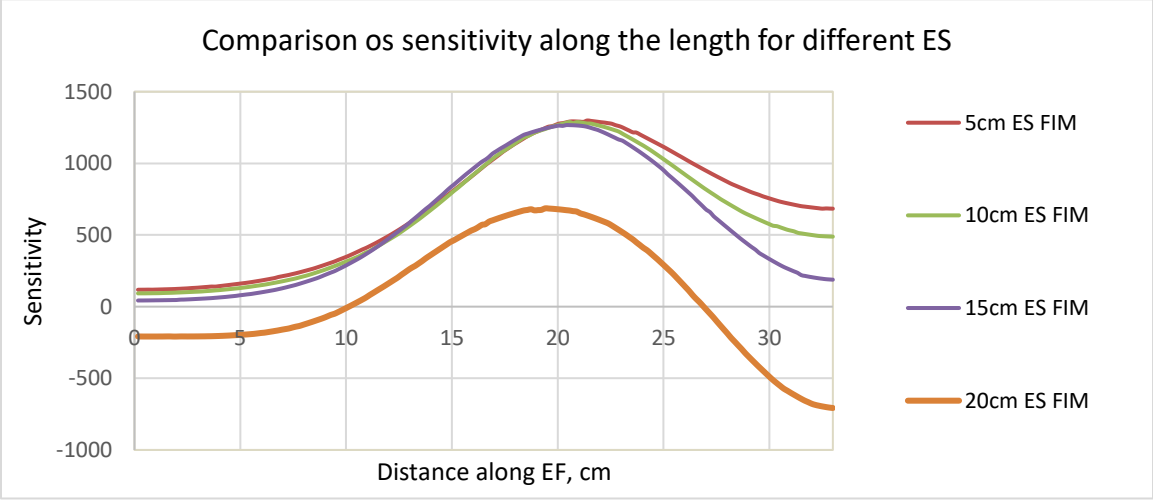

Fig. 5: Sensitivity of FIM along the length (EF) of the phantom for various ES. The midpoint of the electrode configuration is at 20.5cm, around which the peaks occur for all the configurations

3.2 Effect of different electrode widths

Table 4 shows the sensitivity at the center position O in Figure 2b for electrode widths of 0.15cm, 1cm and 3cm respectively. The electrode separation was kept fixed at 15cm. It may be seen that the differences due to different widths of electrodes are negligible.

Table 4: Sensitivity at the center position O (Figure 2b) for different electrode widths. Electrode separation fixed at 15cm.

Electrode Width, cm (ES:15cm)	Sensitivity, arbitrary unit			
	TPIM 1	TPIM 2	FIM Added	FIM Averaged
0.15	508	753	1261	631
1	506	770	1276	638
3	477	807	1284	642

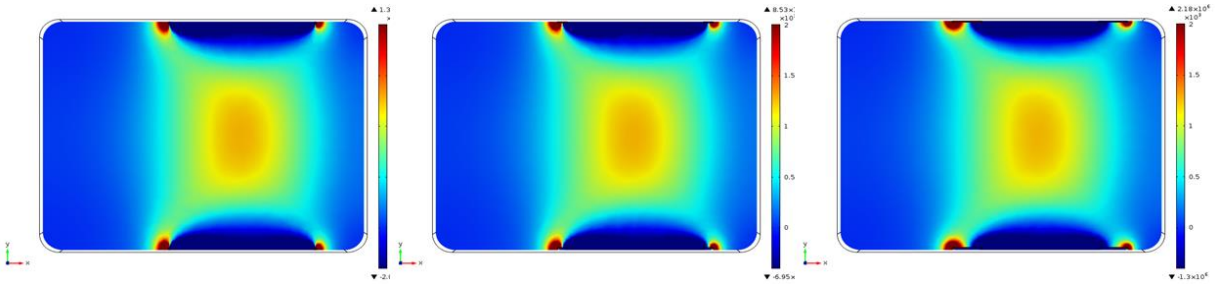

Fig. 6: Distribution of sensitivity of 4-electrode FIM (TPIM1 and TPIM2 added) using 15 cm ES at mid-height (6 cm) for different electrode widths; left: 0.15cm; middle: 1cm; right: 3cm. Sensitivity truncated beyond -400 and 2000 (arbitrary units)

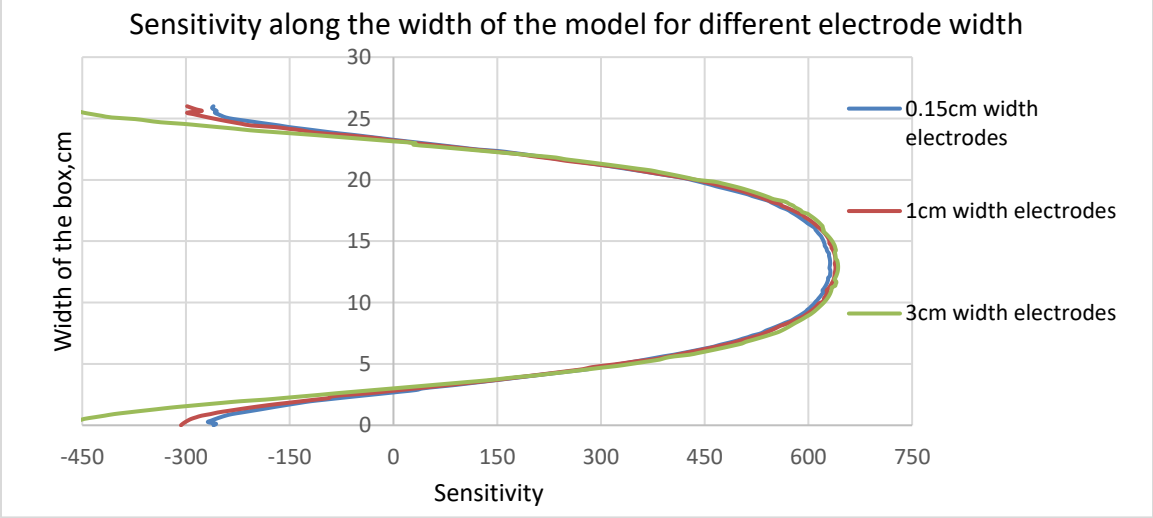

Fig 7: Sensitivity along the width (PQ) of the phantom for electrodes of different widths.

Figure 6 shows colour distributions of the sensitivity of FIM in a horizontal plane at mid height of the phantom. No difference may be observed visually. The sensitivities of FIM along PQ (Figure 2b) for electrodes with different widths are shown in Figure 7. The three sensitivity plots almost overlap in the region of interest (middle of the figure). Only the negative sensitivity values appear to increase with the width of the electrode near the edges (front and back of the phantom).

Figure 8 shows the sensitivity along the length (EF in Figure 2b) of the phantom for electrodes with different widths. Again, the differences are not too great and the peak occurs around 20.5cm, the midpoint of the electrode configuration. The peak shifts slightly towards the right as the width of the electrode increases.

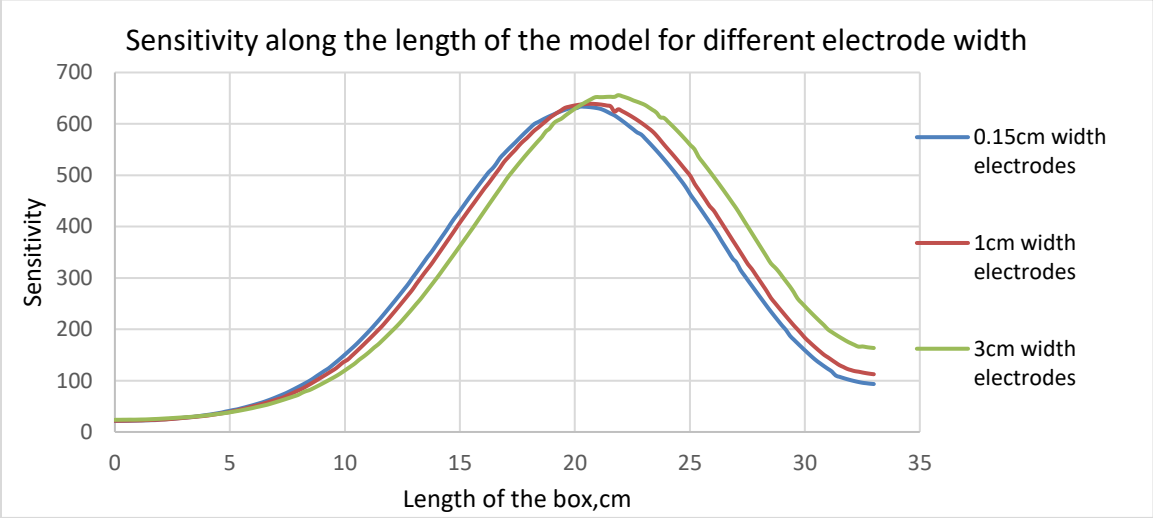

Fig 8: Sensitivity along the length (EF) of the phantom for electrodes with different widths.

4. DISCUSSION

The main aim of the present work was to find optimum values of electrode separation and electrode width in using a 4-electrode FIM technique for probing deep regions of the lung, following new ideas put forward by Rabbani (2018b) for this purpose. In this technique for FIM two electrodes are placed at the front of the thorax and another two at the back in the same horizontal plane to provide a reasonably high sensitivity at the central part of the thorax, which cannot be achieved applying all electrodes one side only. A finite element method was used for this investigation using COMSOL Multiphysics simulation software.

This work was performed on a rounded rectangular phantom representing a thick region of the human thorax, with a width of 33cm, depth 26cm and height 12cm. The choice was also guided by an intent to carry out experimental phantom studies later where such a dimension was practical. In this work, firstly, the separation between each pair of electrodes on the front and on the back (on the 33cm wide sides) were taken as 5cm, 10cm, 15cm and 20 cm to study the effect on deep

sensitivity. For this work, cylindrical electrodes 3cm long with a diameter of 0.3cm were used, the length aligned vertically. Secondly, to study the effects of the width of electrodes, an electrode separation of 15cm was chosen, which was found to be optimum for the particular phantom dimensions through the previous experiment. In this case, the electrodes were flat, with widths 0.15cm, 1cm and 3cm. For all the studies, the electrodes were 3cm long fixed inside the walls of the phantom vertically.

For the study on the effects of electrode separation, it was observed (Table 1) that at the centre point of the electrode configuration, the sensitivity value for TPIM-1 increases with electrode separation while that for TPIM-2 decreases with electrode separation. Values for FIM decrease very little with electrode separation, which is an advantage.

Color sensitivity distributions of 4-electrode FIM for a horizontal plane at the vertical centre of the rectangular phantom as presented in Figure 3 for different electrode separations show that the sensitivity values are very high close to the electrodes and decrease as one goes towards the central region. However, for studies of lungs, these peripheral regions will not be of importance since the region near the electrodes will be occupied by muscles, fat and bones (ribs). For the lung studies, usually the variation in impedance through the breathing cycle is measured taking difference values. It may be expected that the peripheral regions with muscles, fat and bone will not have significant variations under the above conditions and the difference values will be negligible. Therefore, for studies of lung the very high sensitivity near the electrodes is not a point of concern, however, lower values would have been preferable.

Negative sensitivity regions can also be seen in Figure 3 which cannot be avoided for any electrical impedance study that uses TPIM techniques. No easy alternative exists either. Therefore, one needs to understand that the negative sensitivity zones arise in between current and voltage electrodes in TPIM and the electrodes should be placed judiciously so that negative sensitivity zones do not fall on regions that reduce the contribution of the target zone significantly. Furthermore, since FIM adds the sensitivities of the two TPIMs that are aligned orthogonally, the negative sensitivity magnitudes tend to be smaller as the negative sensitivity zones of TPIM-1 fall under the positive sensitivity zones of TPIM-2 and vice versa.

Figure 4 gives a good indication of the desired electrode separations for the specific thorax dimensions used in the present work. For 5cm electrode separation, the variations in sensitivity along the depth is very high, starting from a high negative value near the electrodes, followed by a high positive value and eventually falling to a low value at the centre. The same pattern then repeats on the other side of the thorax, because of symmetry. As the electrode separation increases, the variations are reduced and for 20cm the sensitivity is almost uniform throughout the depth although the values are rather low. For 10cm electrode separation, the values are almost uniform for a range of about 13cm in the central part although there are large negative sensitivity regions near the surfaces on both front and back sides. The values at the central part are also almost double that for 20cm electrode separation. For 15cm separation, the negative sensitivity values are much

reduced near the surfaces while sensitivity in the central part may be considered somewhat uniform although not so uniform as for the 10cm separation.

Again, considering the sensitivity along the width of the thorax as given in Figure 5, an electrode separation of 20cm contributes to less sensitivity in the target zone while having negative sensitivities near both the sides. A separation of 15cm gives the best solution along this axis.

Considering both the above, it appears that electrode separations between 10cm and 15cm should be optimum for a thorax of cross sectional dimension of 33cm×26cm as chosen for this study.

For the studies with different electrode widths as presented in Section 3.2 for widths of 0.15cm, 1cm and 3cm respectively, no significant differences were observed except that the thinnest (0.15cm) had the least negative sensitivity in Figure 7. Therefore, this result would lead to a choice of a width of about 0.15cm.

5. CONCLUSIONS

The results of the present work establishes the new ideas for electrode configurations proposed by Rabbani (2018b) on a stronger footing besides suggesting appropriate electrode separations and electrode widths to be used for a thorax of specified dimensions, which could then be extrapolated to obtain optimum electrode separations and widths for other thorax dimensions, particularly for studies of lung functions where a difference image between inspiration and expiration is of great interest for detection and diagnosis of respiratory problems that are widespread in low and medium income countries like Bangladesh.

ACKNOWLEDGEMENTS

The authors would like to acknowledge the International Science Programme of Uppsala University, Sweden, for partial financial support towards the research work carried out at the department of Biomedical Physics and Technology of the University of Dhaka.

REFERENCES

Barber DC, Brown BH, Freeston IL, 1983. Imaging spatial distributions of resistivity using applied potential tomography. *Electron. Lett. (19) 933–935.*

COMSOL 2022. AC/DC Module Model library manual [Online]. Available: https://www.comsol.com/models

Gabriel, S., Lau, R.W. and Gabriel, C., 1996. The dielectric properties of biological tissues: II. Measurements in the frequency range 10 Hz to 20 GHz. *Physics in medicine & biology*, *41*(11), p.2251.

Geselowitz, D.B., 1971. An application of electrocardiographic lead theory to impedance plethysmography. *IEEE Transactions on biomedical Engineering*, (1), pp.38-41.

Martinsen, O.G. and Grimnes, S., 2011. *Bioimpedance and bioelectricity basics*. Academic press.

Haque, R., Kadir, M.A. and Rabbani, K.S.E., 2019. Probing for stomach using the Focused Impedance Method (FIM). *Journal of Electrical Bioimpedance*, *10*(1), pp.73-82.

Islam, N., Rabbani K.S.E. and Wilson, A., 2010. The sensitivity of focused electrical impedance measurements. *Physiol. Meas.* ***31*** *S97–S109.*

Khalil, S.F., Mohktar, M.S. and Ibrahim, F., 2014. The theory and fundamentals of bioimpedance analysis in clinical status monitoring and diagnosis of diseases. *Sensors*, *14*(6), pp.10895-10928.

Lingwood, B.E., Colditz, P.B. and Ward, L.C., 1999, August. Biomedical applications of electrical impedance analysis. In *ISSPA'99. Proceedings of the Fifth International Symposium on Signal Processing and its Applications (IEEE Cat. No. 99EX359)* (Vol. 1, pp. 367-370). IEEE.

Mobarak, M. and Rabbani, K.S., 2019. Improving the Sensitivity at the E of Lung by using Focused Impedance Method. *SEU Journal of Science and Engineering*, *13*(1), pp.1999-16.

Morucci, J.P. and Rigaud, B., 1996. Bioelectrical impedance techniques in medicine part III: Impedance imaging third section: Medical applications. *Critical Reviews™ in Biomedical Engineering*, *24*(4-6).

Rabbani, K.S.E., 2018a. Focused impedance method: Basics and applications. In *Bioimpedance in biomedical applications and research* (pp. 137-185). Springer, Cham.

Rabbani, K.S.E., 2018b. Simple electrode configurations for probing deep organs using Electrical Bio-Impedance techniques. *Bangladesh Journal of Medical Physics*, *11*(1), pp.1-15.

Rabbani, K.S. and Karal, M.A.S., 2008. A new four-electrode Focused Impedance Measurement (FIM) system for physiological study. *Annals of biomedical engineering*, *36*(6), pp.1072-1077.

Rabbani, K.S.E. and Kadir, M.A., 2011. Possible Applications of Focussed Impedance Method (FIM) in biomedical and other areas of study. *Bangladesh Journal of Medical Physics*, *4*(1), pp.67-74.

Redisch, W., 1971. Electrical impedance plethysmography. *Chest*, *59*(6), p.36.

Sauerheber, R. and Heinz, B., 2015. Temperature effects on conductivity of seawater and physiologic saline, Mechanism and Significance. *Chem. Sci. J*, *6*(109), pp.10-4172.

Thomasset, A., 1963. Bio-electric properties of tissues. Estimation by measurement of impedance of extracellular ionic strength and intracellular ionic strength in the clinic. *Lyon médical, 209, pp.1325-1350.*